AI and Machine Learning for Detecting Myocardial Infarction

Xiantong Xiang

Shandong University

Tuesday, November 5th, 2024

Contents

背景

- 心血管疾病早期诊断的高误诊率和潜在患者的发现
- 深度学习与人工智能的应用
- 数据和隐私问题
- 便携式和可穿戴设备的普及
- 心电图（ECG）是诊断心血管疾病最常见、低成本且便捷的工具

ECG-Based Deep Learning and Clinical Risk Factors to Predict Atrial Fibrillation

- **Objectives**:to infer 5-year incident AF risk using 12-lead ECGs in patients receiving longitudinal primary care at Massachusetts General Hospital (MGH).
- **Method**:Convolutional neural network (ECG-AI)
- **Innovation Point**:
  - Artificial intelligence–based analysis of 12-lead ECGs has similar predictive usefulness as an established clinical risk factor model for incident atrial fibrillation (AF), and both are complementary.
  - An ECG–artificial intelligence model for AF had predictive usefulness across independent study samples, discriminated risk in patients with heart failure and stroke, and was applicable to single-lead ECG tracings.

Circulation,Q1,B1,IF35.5,2022,DOI: 10.1161/CIRCULATIONAHA.121.057480,PMID: 34743566

A Novel ECG-Based Deep Learning Algorithm to Predict Cardiomyopathy in Patients With Premature Ventricular Complexes

- **Objectives**:aims to assess a deep-learning model to predict cardiomyopathy among patients with PVCs.
- **Method**:the largest available pretrained ResNet model (ResNet-152)
- ECG data consists of XML files containing waveform data for leads I, II, and V1V6. The remaining leads (III, aVF, aVL, and aVR) are called "derived leads" in that they only contain information present within other leads.
- ECG waveforms were subject to noise reduction by applying the Butterworth Bandpass filter, followed by a median filter.
- Resulting waveform data were plotted to images to allow use of 2-dimensional convolutional neural networks.

JACC Clin Electrophysiol,Q1,B1,IF8.0,2023,DOI:10.1016/j.jacep.2023.05.025,PMID: 37480862

- **Major Contributions**:
  - the signals of each patient are grouped to ensure that they can only be assigned to one of the partitions
  - a different combination of Principal Component Analysis (PCA) and Discrete Wavelet Transform (DWT)
  - By utilizing end-to-end deep neural networks, we are able to build efficient models that require only few steps to detect and localize MI from the raw signals.
- **Method**:
  - a classic ECG processing method with a novel configuration including a shallow neural network (NN)
  - an end-to-end convolutional neural network

Applied Soft Computing,Q1,B1,IF7.2,2020,DOI: 10.1016/j.asoc.2020.106383

Deep Learning for Premature Ventricular Contraction-Cardiomyopathy: Are We Digging Deep Enough?

- SHOULD THE MODEL INPUT BE MATRICES OR IMAGES ?
  - Lampert et al did start out with ECG waveform data but later plotted them as images.
  - Though this conversion facilitates human comprehension, it is an extraneous step that inadvertently confines the AI to human-like processing.
  - Liberating the AI from such human-oriented constraints could potentially lead to more optimal outcomes.
  - The conversion introduces an unnecessary restriction in the form of image resolution and generates an excess of superfluous white pixels surrounding the ECG tracing.
  - Consequently, it can be questioned whether this is worth the additional computational currency.

JACC Clin Electrophysiol,Q1,B1,IF8.0,2023,DOI:10.1016/j.jacep.2023.07.003,PMID: 37611994

Deep Learning of Electrocardiograms in Sinus Rhythm From US Veterans to Predict Atrial Fibrillation

- **Input**:ECG waveform data was acquired at 250 Hz and extracted as 10 second, 12 x 2500 matrices of amplitude values, stored as base64 text. ECGs underwent baseline wander correction using median filtering at 200ms and 600ms intervals and z-score normalization.
- **Method**: an atrous convolutional neural network

JAMA Cardiol,Q1,B1,IF14.8,2023,DOI:10.1001/jamacardio.2023.3701,PMID: 37851434

Development and validation of machine learning algorithms based on electrocardiograms for cardiovascular diagnoses at the population level

- **Objectives**: while existing studies have mainly concentrated on individual labels, there hasn’t been any prior research developing a predictive system for the simultaneous detection of these specific conditions.
- **Method**: ResNet-based deep learning (DL) using ECG tracings and extreme gradient boosting (XGB) using ECG measurements.

NPJ Digit Med,Q1,B1,IF12.4,2024,DOI:10.1038/s41746-024-01130-8.PMID: 38762623

A deep learning algorithm for detecting acute myocardial

- **Objectives**: aim to develop a deep learning model (DLM) as a diagnostic support tool based on a 12-lead electrocardiogram.
- **Innovation Point**:
  - Integration of a DLM may assist frontline physicians in recognising AMI in a timely and precise manner to prevent delayed diagnosis or misdiagnosis of AMI and thereby provide prompt reperfusion therapy.
  - The diagnostic power for STEMI and NSTEMI by the DLM and conventional cardiac troponin I (cTnI) was also evaluated.

EuroIntervention,Q1,B1,IF7.6,2021,DOI:10.4244/eij-d-20-01155,PMID: 33840640

Machine learning for diagnosis of myocardial infarction using cardiac troponin concentrations

- **Objectives**: to identify patients with an adjudicated diagnosis of type 1, type 4b or type 4c myocardial infarction during the index hospital admission.
- **Methods**: Four statistical methods
  - Logistic Regression
  - Naive Bayes
  - Random Forest
  - Extreme Gradient Boosting (XGBoost)

Nature Medicine,Q1,B1,IF58.7,2023,GSID: nWVNwATkyUAJ

Machine learning for ECG diagnosis and risk stratification of occlusion myocardial infarction

- **Objectives**:
  - identify the most important ECG features driving the classifications
  - OMI risk score provides enhanced rule-in and rule-out accuracy
- **Methods**: fit 10 machine learning classifiers
  - regularized logistic regression
  - linear discriminant analysis
  - support vector machine (SVM)
  - Gaussian naive Bayes
  - Random Forest
  - gradient boosting machine
  - extreme gradient boosting
  - stochastic gradient descent logistic regression
  - k-nearest neighbors
  - artificial neural networks

Nature Medicine,Q1,B1,IF58.7,DOI:2023,10.1038/s41591-023-02396-3,GSID: dqWsaQy__DA8J

Bimodal Masked Autoencoders with Internal Representation Connections for Electrocardiogram Classification

- **Background**: the majority of methods concentrate solely on time domain information, overlooking the information originating from additional modalities or perspectives.
- **Method**: a novel bimodal masked autoencoder framework (BMIRC)
- **Innovation Point**:
  - a novel bimodal masked autoencoder framework for time-frequency joint modeling
  - internal representation connections (IRC) from the encoder to the decoder

Bimodal Masked Autoencoders with Internal Representation Connections for Electrocardiogram Classification

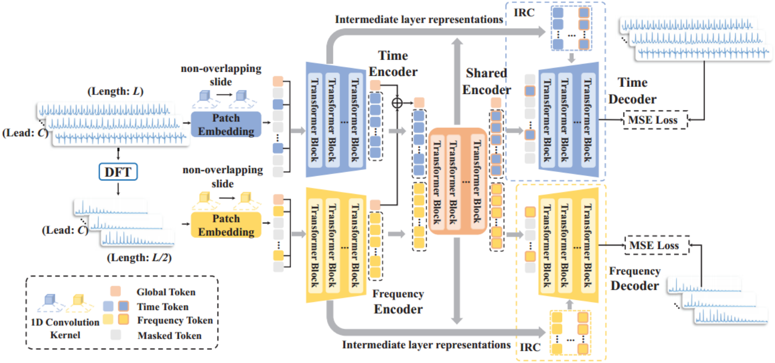

- $ECG(Time) \xrightarrow{DFT} ECG(Frequency)$
- $ECG(T\&F) \Rightarrow Encoder(T\&F) \Rightarrow Encoder(Shared) \Rightarrow Decoder \Leftarrow IRC$

- The tokens of T and F can be expressed as

$$Z_t = [z_t^1, z_t^2, \dots, z_t^{\frac{L}{S}}] \in \mathbb{R}^{\frac{L}{S} \times D}$$

$$Z_f = [z_f^1, z_f^2, \dots, z_f^{\frac{L}{2S}}] \in \mathbb{R}^{\frac{L}{2S} \times D}$$

- learnable position embeddings $\mathrm{PE} \in \mathbb{R}^{N \times D}$ are integrated into the patch embeddings

$$\tilde{I}_m = Z_m + \mathrm{PE}_m$$

$$I_m = \mathrm{Concat}(z_g^m, \tilde{I}_m)$$

- a random masking strategy, meaning that each token has the same probability of being masked.

Bimodal Masked Autoencoders with Internal Representation Connections for Electrocardiogram Classification

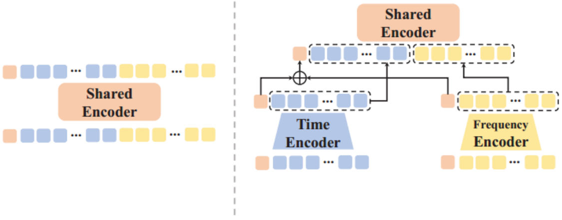

(a) All Shared (b) Specific-Shared(Ours)

- the global tokens of time and frequency modalities are added and inserted at the first position of the sequence, with the other tokens concatenated sequentially.

$$\tilde{O}_m = LN(O_m) = [\tilde{o}_g^m, \tilde{o}_1^m, \tilde{o}_2^m, \ldots, \tilde{o}_n^m]$$

$$O_0^s = [o_g^t + \tilde{o}_g^f, \tilde{o}_1^t, \tilde{o}_2^t, \ldots, \tilde{o}_n^t, \tilde{o}_1^f, \tilde{o}_2^f, \ldots, \tilde{o}_n^f]$$

$$O_s = \Theta(O_0)$$

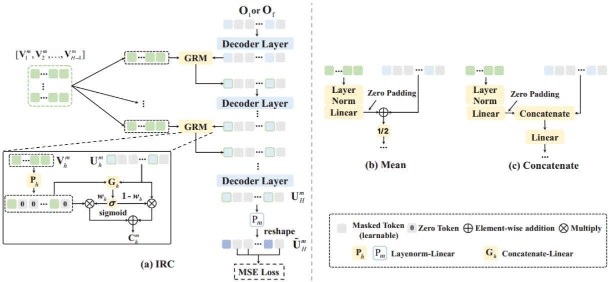

- gated representation mixer called GRM

$$\hat{V}_h = P_h(V_h)$$

$$w_h = \sigma(G_h(\hat{V}_h, U_h^m))$$

$$C_h^m = w_h * \hat{V}_h + (1 - w_h) * U_h^m$$

$$U_{h+1}^m = \Lambda_{h+1}(C_h^m)$$

- **Datasets**:
  - Ningbo dataset (from Ningbo First Hospital)
  - PTBXL dataset (from Physikalisch-Technische Bundesanstalt)
  - Chapman dataset (from Chapman University, Shaoxing People’ s Hospital)
  - Georgia
  - Hefei

- **Baselines:**
  - TF-C 在三个不同的域（时间域、频率域和时频域）中执行对比学习，以获得可迁移的表示。
  - TS-TCC 通过跨视图预测学习稳健的时间表示，并在不同视图之间进行对比学习，以增强模型的可辨别性
  - CPC 通过利用当前时间步的上下文表示来预测后续时间步的表示，专注于时间不变性
  - TimesURL 引入了一种基于频率-时间的增强方法，旨在保留时间特性，同时将时间重构作为与对比学习的联合优化目标
  - SimMTM 结合了流形学习用于掩码重构，通过加权聚合流形外的多个邻居来恢复被掩盖的时间点
  - PatchTST 将时间序列划分为多个片段，并在预训练阶段采用掩码数据重构任务
  - TimeMAE 采用窗口切片策略处理时间序列，并结合了两种任务：掩码表示回归和掩码码字分类，从而促进表示学习

Intra-Domain Evaluation

Models	Ningbo				PTB-XL				Chapman			
	ACC	F1	AUROC	AUPRC	ACC	F1	AUROC	AUPRC	ACC	F1	AUROC	AUPRC
TF-C_I	55.87	75.30	92.83	49.90	51.08	78.84	91.06	53.58	59.59	77.10	91.89	51.84
TF-C_R	57.58	76.92	92.27	50.25	50.05	77.61	88.24	49.70	60.57	76.74	89.59	52.27
TS-TCC_I	61.07	81.79	92.61	53.72	55.75	81.23	88.42	50.60	61.69	78.29	89.18	46.28
TS-TCC_R	61.05	81.66	93.69	57.59	57.67	82.12	90.28	53.37	**64.81**	**81.11**	**92.65**	**55.39**
CPC	59.26	79.32	95.25	56.08	55.24	80.61	93.14	55.03	59.25	75.97	91.97	46.33
TimesURL	59.43	81.20	94.50	53.49	53.85	80.04	91.23	50.99	55.44	75.96	89.99	48.13
$SimMTM_D$	54.85	75.67	90.79	44.68	52.98	78.84	87.17	45.03	45.88	61.12	86.43	38.50
$SimMTM_R$	55.02	74.10	91.48	49.36	54.67	80.43	85.80	47.24	59.44	75.74	88.25	47.03
PatchTST	55.28	77.05	93.47	50.07	54.90	80.40	90.64	50.05	53.34	73.93	91.21	49.28
TimeMAE	57.76	79.97	93.55	54.30	54.05	80.32	90.49	49.91	57.20	74.58	86.82	46.81
Random Init	59.30	79.76	93.16	52.17	54.17	79.59	89.69	48.98	61.30	78.66	86.71	50.28
BMIRC(Ours)	**63.76**	**84.30**	**95.78**	**61.17**	**57.78**	**82.46**	**93.32**	**55.81**	62.42	80.51	90.06	52.05

- BMIRC 在宁波和 PTB-XL 数据集上表现优于所有基线方法，但在 Chapman 数据集上的表现略微逊色
- 随着数据集规模的扩大，BMIRC 相较于基线方法的性能提升也逐渐增加
- 虽然 BMIRC 在 Chapman 数据集上的整体表现不及 TS-TCCR，他们认为通过迁移学习可以改变这一情况
- 与未使用预训练权重的随机初始化（Random Init）相比 BMIRC 表现出显著优势

Cross-Domain Evaluation

Models	Ningbo→PTB-XL				Ningbo→Chapman				PTB-XL→Chapman			
	ACC	F1	AUROC	AUPRC	ACC	F1	AUROC	AUPRC	ACC	F1	AUROC	AUPRC
TF-C_I	50.92	78.33	89.95	52.93	58.66	76.45	92.25	54.12	59.79	76.98	92.52	53.92
TF-C_R	48.47	77.56	88.23	50.22	58.76	76.50	87.83	47.99	59.15	76.53	88.01	48.08
TS-TCC_I	54.92	80.11	89.78	51.39	63.06	79.59	89.64	50.17	62.66	79.31	90.61	49.01
TS-TCC_R	56.20	82.17	91.71	53.79	63.79	80.10	91.71	56.04	**65.40**	80.99	91.67	**56.13**
CPC	55.79	81.13	92.87	54.99	59.79	76.82	93.25	47.96	58.96	76.15	93.30	50.26
TimesURL	54.42	80.26	91.24	51.46	58.13	77.03	89.85	48.35	61.44	77.61	89.96	49.34
$SimMTM_D$	53.11	78.36	87.36	45.19	46.07	60.61	85.77	37.78	49.93	65.71	87.01	39.30
$SimMTM_R$	53.96	79.87	86.79	47.39	60.52	77.08	88.54	46.86	60.57	77.02	88.56	46.64
PatchTST	54.97	80.68	90.83	50.22	57.54	75.80	92.16	50.69	49.00	69.75	88.59	47.11
TimeMAE	56.41	81.67	91.62	53.21	60.96	78.54	91.17	52.45	56.03	74.20	90.05	48.96
BMIRC(Ours)	**57.23**	**82.57**	**93.13**	**56.54**	**65.20**	**82.27**	**94.38**	**58.66**	64.76	**81.59**	**93.78**	54.14

- 在大多数场景中，BMIRC 超过基线。对于 Chapman 数据集，采用来自较大数据集的预训练权重显著增强了大多数模型的性能
- 更大的预训练数据集对应着更显著的改进
- BMIRC 可以通过在大型数据集上进行广泛的预训练提高其泛化能力

Fine-tuning with More Downstream Datasets

Models	Pretraining Datasets	Georgia				Hefei			
		ACC	F1	AUROC	AUPRC	ACC	F1	AUROC	AUPRC
RandomInit	–	32.80	49.75	84.77	39.81	66.80	85.60	92.34	39.24
TS-TCC$_R$	Ningbo	37.66	57.44	87.10	47.19	74.57	90.15	92.70	45.24
BMIRC(Ours)	Ningbo	37.17	58.30	<u>91.36</u>	49.28	<u>75.47</u>	<u>90.72</u>	<u>94.90</u>	45.95
TS-TCC$_R$	Ningbo, PTB-XL, Chapman	<u>38.58</u>	<u>58.57</u>	88.54	<u>50.22</u>	75.14	90.32	90.83	<u>48.49</u>
BMIRC(Ours)	Ningbo, PTB-XL, Chapman	**40.48**	**61.83**	**91.49**	**51.09**	**77.09**	**91.63**	**95.67**	**49.43**

- BMIRC 在这些下游任务上的表现优于 baselines，更大的预训练数据集与更高的性能相关

Fine-tuning with Different Proportions of Training Set

Models	25%				50%				75%				100%			
	ACC	F1	AUROC	AUPRC	ACC	F1	AUROC	AUPRC	ACC	F1	AUROC	AUPRC	ACC	F1	AUROC	AUPRC
								Ningbo(intra-domain)								
TF-C_I	53.76	71.76	89.58	41.21	56.94	76.17	92.05	47.16	56.01	75.48	92.38	48.54	55.87	75.30	92.83	49.90
TF-C_R	55.98	74.78	87.01	41.13	54.40	74.26	88.49	46.95	58.56	77.89	90.88	48.81	57.58	76.92	92.27	50.25
TS-TCC_I	58.23	79.09	89.15	42.92	56.45	78.25	91.26	48.54	61.01	81.62	92.65	51.97	61.07	81.79	92.61	53.72
TS-TCC_R	**59.06**	**79.33**	**91.43**	**48.49**	60.66	81.38	93.11	52.06	61.54	81.84	93.50	53.80	61.05	81.66	93.69	57.59
CPC	48.17	66.71	86.19	29.69	55.82	76.01	91.84	44.65	58.20	78.31	94.65	52.30	59.26	79.32	95.25	56.08
TimesURL	50.74	74.42	88.58	41.74	55.08	77.98	91.67	47.85	56.80	79.59	93.20	50.41	59.43	81.20	94.50	53.49
$SimMTM_D$	42.29	58.21	84.56	30.32	50.80	70.09	87.98	38.87	54.18	73.98	89.80	42.94	54.85	75.67	90.79	44.68
$SimMTM_R$	51.24	69.25	86.58	35.82	57.57	77.90	89.09	43.59	56.04	76.12	90.96	45.93	55.02	74.10	91.48	49.36
PatchTST	49.26	71.62	89.20	42.39	51.96	74.29	89.32	46.35	53.83	75.76	91.95	48.44	55.28	77.05	93.47	50.07
TimeMAE	51.47	73.52	86.24	44.02	53.26	74.61	89.91	48.90	56.50	77.18	92.56	51.42	57.76	79.97	93.55	54.30
Random Init	54.36	75.72	85.22	41.66	57.53	78.89	86.98	47.24	57.07	78.14	92.06	50.57	59.30	79.76	93.16	52.17
BMIRC(Ours)	57.99	78.94	90.80	45.86	**61.87**	**83.06**	**94.91**	**53.11**	**62.97**	**83.55**	**95.58**	**56.28**	**63.76**	**84.30**	**95.78**	**61.17**
								Ningbo→Chapman(cross-domain)								
TF-C_I	51.73	67.03	84.24	34.88	56.91	73.97	89.06	45.29	57.25	74.08	90.83	50.07	58.66	76.45	92.25	54.12
TF-C_R	53.93	70.39	83.09	34.90	56.71	74.16	85.58	42.16	58.47	76.12	88.01	46.11	58.76	76.50	87.83	47.99
TS-TCC_I	60.42	76.83	87.03	42.02	59.05	77.11	88.99	45.52	62.27	79.11	89.70	49.30	63.06	79.59	89.64	50.17
TS-TCC_R	61.74	78.60	89.26	45.97	64.03	80.49	90.28	49.94	63.54	80.56	91.20	54.72	63.79	80.10	91.71	56.04
CPC	50.85	69.31	86.87	37.23	53.49	71.82	88.37	39.61	58.17	75.39	91.61	45.26	59.79	76.82	93.25	47.96
TimesURL	56.27	73.40	84.79	41.35	59.10	76.25	86.02	44.78	58.37	76.99	87.05	46.61	58.13	77.03	89.85	48.35
$SimMTM_D$	27.33	34.01	69.75	17.56	32.06	43.21	81.54	28.66	45.14	59.48	85.66	36.20	46.07	60.61	85.77	37.78
$SimMTM_R$	27.96	35.85	76.04	23.73	50.27	66.25	85.21	37.37	57.59	73.98	87.26	45.61	60.52	77.08	88.54	46.86
PatchTST	44.41	62.32	85.88	36.37	48.66	69.87	90.00	44.62	52.81	73.22	89.99	49.40	57.54	75.80	92.16	50.69
TimeMAE	49.34	67.31	85.06	42.03	54.95	73.20	88.00	46.31	56.91	74.33	89.18	49.34	60.96	78.54	91.17	52.45
Random Init	56.12	73.48	83.36	41.46	59.59	76.86	84.81	44.89	61.20	78.39	85.86	47.52	61.30	78.66	86.71	50.28
BMIRC(Ours)	**62.03**	**79.22**	**91.19**	**46.85**	**64.81**	**82.25**	**94.08**	**54.11**	**64.47**	**81.96**	**94.82**	**58.77**	**65.20**	**82.27**	**94.38**	**58.66**

Fine-tuning with Different Proportions of Training Set

- 评估了在微调阶段使用不同比例的训练集（25%、50%、75%、100%）对模型性能的影响
- BMIRC 在大多数场景中都优于所有基线，仅在使用宁波数据集的 25% 时表现不及 TS-TCCR
- 随着有标签数据量的增加或在跨域设置下，BMIRC 持续优于 TS-TCCR
- 随着训练集比例的增加，基线模型的性能逐渐提高，但性能提升的幅度逐渐放缓
- BMIRC 在下游任务标签稀疏时也能取得令人满意的结果

Analysis of the Bimodal Masking Rates

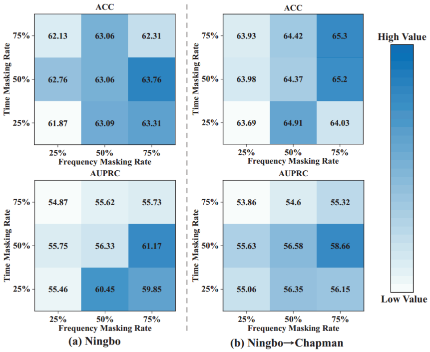

- 频率模态掩蔽率的增加对应于模型性能的逐渐改善
- 保持频率模态中的掩蔽率恒定，经常观察到模型性能在时间模态中的 50% 的掩蔽率处达到其峰值
- 最佳配置被确定为时间模态掩蔽率为 50%，频率模态掩蔽率为 75%

Analysis of the Bimodal Reconstruction Loss Weights

Parameters	Ningbo				Ningbo→Chapman			
	ACC	F1	AUROC	AUPRC	ACC	F1	AUROC	AUPRC
$\alpha = 0.6, \beta = 1.4$	63.67	84.06	95.09	55.57	64.47	81.97	92.98	55.35
$\alpha = 0.8, \beta = 1.2$	63.39	84.16	94.37	56.08	64.37	81.56	93.91	54.94
$\alpha = 1.0, \beta = 1.0$	**63.76**	**84.30**	95.78	**61.17**	**65.20**	**82.27**	**94.38**	**58.66**
$\alpha = 1.2, \beta = 0.8$	63.07	83.82	**95.87**	55.71	64.52	81.65	92.23	55.16
$\alpha = 1.4, \beta = 0.6$	63.49	84.05	95.30	57.38	64.47	81.62	93.98	56.49

- 当 α 和 β 都设置为 1.0 时，模型的性能达到最佳，表明两种模态的重建损失权重同等重要

Analysis of the Sampling Rate of ECG

Parameters	Ningbo				Ningbo→Chapman			
	ACC	F1	AUROC	AUPRC	ACC	F1	AUROC	AUPRC
fs = 50Hz	**64.00**	**84.39**	95.63	56.86	64.37	82.23	92.60	58.18
fs = 100Hz	63.76	84.30	**95.78**	**61.17**	**65.20**	**82.27**	**94.38**	**58.66**
fs = 200Hz	62.99	83.69	94.37	58.88	64.76	82.10	91.60	55.99

- 随着输入长度从 500 增加到 1000，模型性能有所提升，但更大的输入长度（2000）并未带来更好的性能
- 过多的数据冗余对模型学习是有害的

The Effects of Additional Frequency Modality

Scenarios	w/o frequency				w/o IRC				Full Model (Ours)			
	ACC	F1	AUROC	AUPRC	ACC	F1	AUROC	AUPRC	ACC	F1	AUROC	AUPRC
Ningbo	57.16	77.29	92.96	52.53	63.09	84.01	95.23	56.72	**63.76**	**84.30**	**95.78**	**61.17**
PTB-XL	54.81	80.35	90.18	50.37	56.07	82.19	93.12	54.93	**57.78**	**82.46**	**93.32**	**55.81**
Chapman	52.17	70.82	89.75	47.94	**63.10**	80.09	**91.14**	50.35	62.42	**80.51**	90.06	**52.05**
Ningbo→PTB-XL	55.27	81.01	90.23	51.09	56.80	82.09	**93.46**	55.35	**57.23**	**82.57**	93.13	**56.54**
Ningbo→Chapman	55.73	73.68	91.67	50.18	64.81	82.15	92.97	56.49	**65.20**	**82.27**	**94.38**	**58.66**
PTB-XL→Chapman	54.37	73.36	89.81	48.58	64.13	81.56	92.63	54.05	**64.76**	**81.59**	**93.78**	**54.14**

- 当去除频率模态时，所有场景的性能都出现了显著下降
- 去除频率模态会削弱模型提取判别性表示的能力，最终导致性能下降

The Effects of Bimodal Joint Encoder

Scenarios	All-Shared				Specific-Shared (Ours)			
	ACC	F1	AUROC	AUPRC	ACC	F1	AUROC	AUPRC
Ningbo	62.86	83.89	95.75	60.48	**63.76**	**84.30**	**95.78**	**61.17**
PTB-XL	57.67	**82.54**	92.92	55.74	**57.78**	82.46	**93.32**	**55.81**
Chapman	61.25	79.10	**91.68**	51.35	**62.42**	**80.51**	90.06	**52.05**
Ningbo→PTB-XL	57.21	82.52	**93.73**	56.29	**57.23**	**82.57**	93.13	**56.54**
Ningbo→Chapman	**65.30**	**82.44**	**95.25**	**58.72**	65.20	82.27	94.38	58.66
PTB-XL→Chapman	63.45	81.30	93.59	**55.18**	**64.76**	**81.59**	**93.78**	54.14
Average Rank	1.83	1.67	1.50	1.67	**1.17**	**1.33**	1.50	**1.33**

- Specific-Shared 架构在大多数场景中优于 All Shared 架构，仅在 Ningbo→Chapman 场景中略微表现不佳
- Specific-Shared 架构在 ACC、F1 和 AUPRC 指标上显示出优于 All Shared 架构的表现，而在 AUROC 指标上则保持了相当的表现

The Effects of IRC

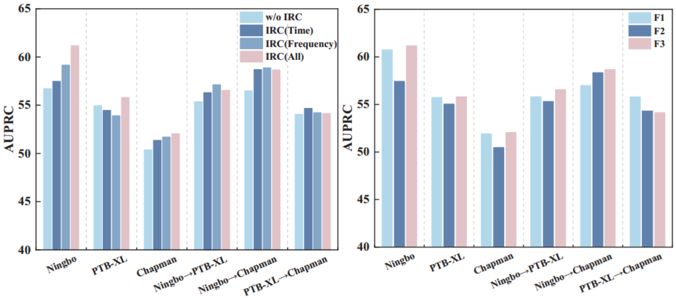

- 在大多数场景中，IRC 的整合都带来了性能提升，突显了其有效性
- 在域内设置下，IRC(All) 一贯表现优于其他选项。尽管在跨域设置下 IRC(All) 未达到最佳结果，但其性能接近最优
- F3 在大多数场景中取得了最佳性能，仅在 PTB-XL→Chapman 场景中表现较差。F2 的整体性能最差

The Effects of GRM

Scenarios	Mean				Concatenate				GRM(Ours)			
	ACC	F1	AUROC	AUPRC	ACC	F1	AUROC	AUPRC	ACC	F1	AUROC	AUPRC
Ningbo	61.64	83.44	95.42	57.71	63.44	84.04	**95.81**	57.69	**63.76**	**84.30**	95.78	**61.17**
PTB-XL	57.35	**82.51**	92.82	55.59	57.69	82.34	92.63	54.00	**57.78**	82.46	**93.32**	**55.81**
Chapman	62.13	80.10	89.34	50.70	**63.06**	80.50	**90.22**	51.57	62.42	**80.51**	90.06	**52.05**
Ningbo→PTB-XL	**57.85**	**82.66**	**93.90**	55.50	57.51	82.64	93.25	**56.86**	57.23	82.57	93.13	56.54
Ningbo→Chapman	64.81	82.05	93.93	56.87	**66.03**	**82.77**	94.00	**59.32**	65.20	82.27	**94.38**	58.66
PTB-XL→Chapman	64.62	**81.79**	92.64	**56.57**	64.18	80.87	91.81	53.70	**64.76**	81.59	**93.78**	54.14
Average Rank	2.50	2.00	2.33	2.33	1.83	2.17	2.00	2.17	**1.67**	**1.83**	**1.67**	**1.50**

- GRM 独特的自适应选通融合策略可以增强模型的泛化能力

ECG

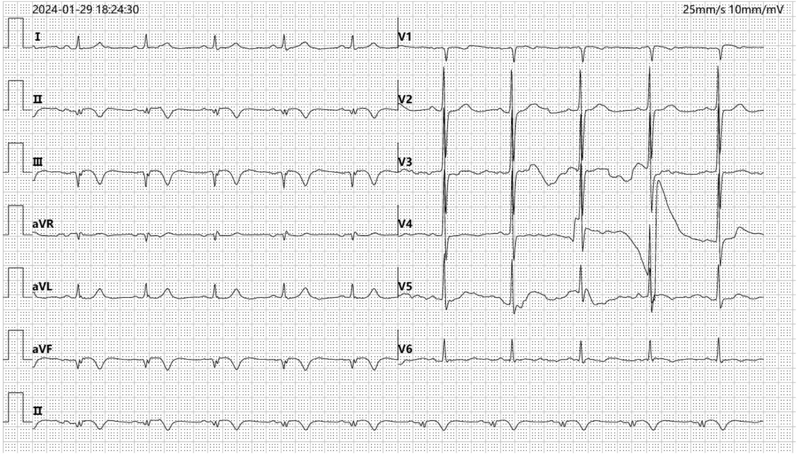
2024-01-29 18:24:30
25mm/s 10mm/mV
I
II
III
aVR
aVL
aVF
II
V1
V2
V3
V4
V5
V6

ECG

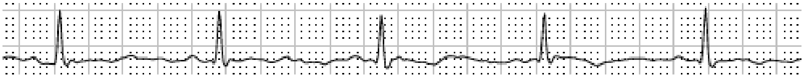

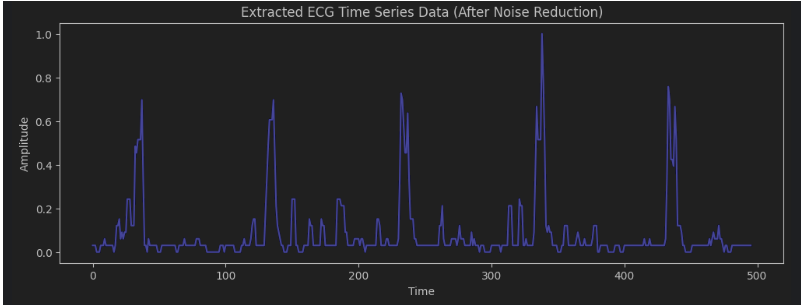
Extracted ECG Time Series Data (After Noise Reduction)
Amplitude
1.0
0.8
0.6
0.4
0.2
0.0
0
100
200
300
400
500
Time

ECG

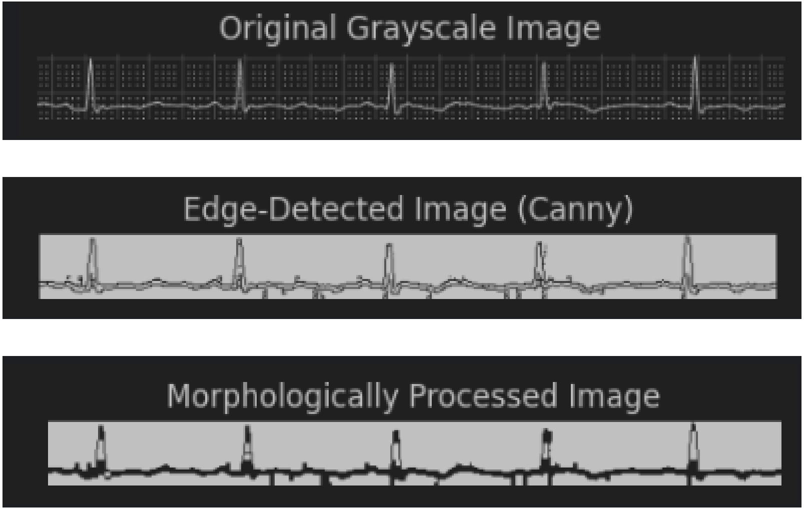
Original Grayscale Image
Edge-Detected Image (Canny)
Morphologically Processed Image

ECG

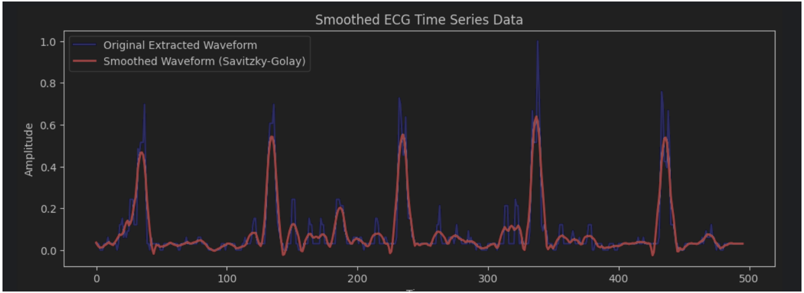
Smoothed ECG Time Series Data
Original Extracted Waveform
Smoothed Waveform (Savitzky-Golay)
Amplitude
1.0
0.8
0.6
0.4
0.2
0.0
0
100
200
300
400
500

ECG

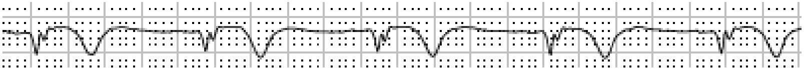

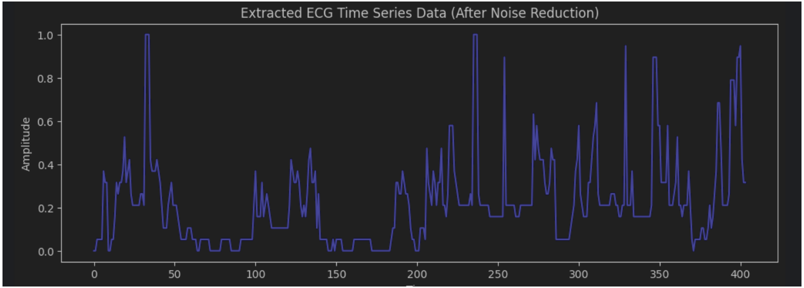
Extracted ECG Time Series Data (After Noise Reduction)
Amplitude
1.0
0.8
0.6
0.4
0.2
0.0
0
50
100
150
200
250
300
350
400

ECG

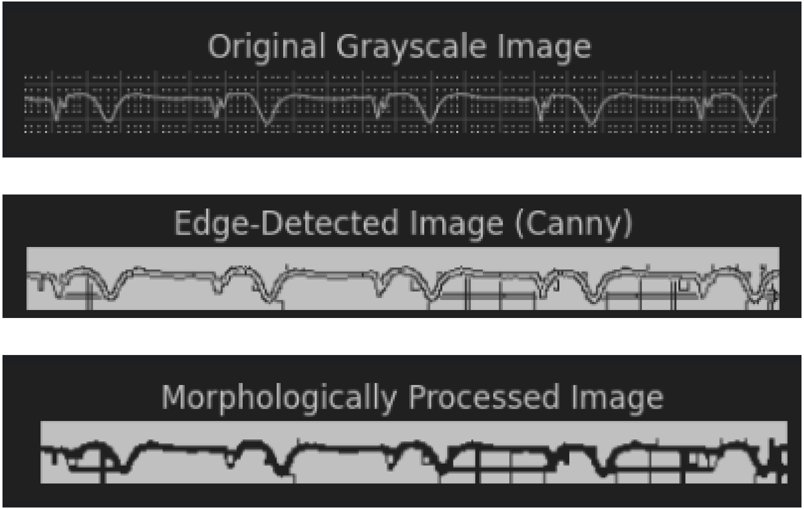
Original Grayscale Image
Edge-Detected Image (Canny)
Morphologically Processed Image

ECG

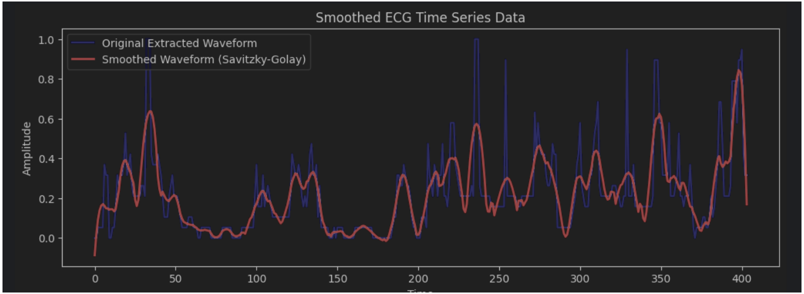
Smoothed ECG Time Series Data
Original Extracted Waveform
Smoothed Waveform (Savitzky-Golay)
Amplitude
1.0
0.8
0.6
0.4
0.2
0.0
0
50
100
150
200
250
300
350
400

目前遇到的问题

- 从二维 ECG 图像提取一维时间序列数据受到的背景噪声影响太大，提取的效果并不稳定
- 提取出来的数据与真实数据的误差不可避免，容易对后续研究造成影响
- 截取的 ECG 曲线没有横纵坐标尺度标准，提取出来的一维时间序列数据缺少标准
- 原始数据存在 ECG 曲线相互交错的问题，影响较大，很难解决